

## Room-temperature ferromagnetism in $\text{Ge}_{1-x}\text{Mn}_x$ nanowires

Olga Kazakova,<sup>1,\*</sup> Jaideep S. Kulkarni,<sup>2</sup> Justin D. Holmes,<sup>2</sup> and Sergej O. Demokritov<sup>3</sup>

<sup>1</sup>National Physical Laboratory, Teddington, United Kingdom

<sup>2</sup>Materials Section and Supercritical Fluid Centre, Department of Chemistry, University College Cork, Cork, Ireland

<sup>3</sup>Institute of Applied Physics, Westfälische Wilhelms-University Münster, Germany

(Received 7 June 2005; published 14 September 2005)

We report an observation of room temperature ferromagnetism in Ge nanowires doped with Mn. High-density arrays of  $\text{Ge}_{1-x}\text{Mn}_x$  ( $x=1\% - 5\%$ ) nanowires with the smallest diameter of 35 nm have been synthesized within the pores of anodized aluminium oxide membranes using a supercritical fluid inclusion-phase technique. Structural analysis of the nanowires proved the existence of a highly crystalline germanium host lattice containing discrete manganese atoms. All of the nanowires studied displayed ferromagnetic properties at room temperature. Ferromagnetic ordering reaches a maximum at intermediate Mn concentrations. The magnetic properties of the nanowires can be understood by considering the influence of co-dopant nonmagnetic impurities and nanowire/membrane interfaces.

DOI: 10.1103/PhysRevB.72.094415

PACS number(s): 75.50.Pp, 75.75.+a

### I. INTRODUCTION

The injection of spin-polarized current into nonmagnetic semiconductors has recently attracted great interest due to its potential application in spintronics.<sup>1</sup> Spintronics requires fabrication of ferromagnetic nanostructures that can transport spin-polarized carriers at room temperature, be electrically tunable, and can be assembled on a microscopic chip, i.e., be easily compatible with existing silicon manufacturing technologies. The most direct method to induce spin-polarized electrons into a semiconductor is by introducing appropriate transition metal dopants (such as Mn, Fe, Co) at level of a few percent, producing a dilute magnetic semiconductor (DMS).<sup>1-4</sup> Extensive research has been carried out in order to create DMS materials with well-established room temperature ferromagnetism. Despite several encouraging results, DMS materials are still struggling to reliably achieve the desired high Curie temperature,  $T_c$ . For example,  $T_c$  above room temperature was first theoretically predicted in GaN:Mn by the hole-mediated exchange interaction model<sup>5</sup> and later observed experimentally in thin film samples.<sup>6</sup> During the last few years the high-temperature ferromagnetism was observed in a variety of wide bandgap semiconductors, including AlN, GaP, and SiC, doped with the whole range of transition metals, i.e., Cr, Mn, Fe, Co, and Ni.<sup>7-10</sup> The existence of room temperature ferromagnetism in Mn-doped GaN nanostructures, e.g., nanowires, was recently reported.<sup>11,12</sup>

Conversely, room-temperature ferromagnetism in narrow-band gap group IV semiconductors (like  $\text{Ge}_{1-x}\text{Mn}_x$ ) is not expected. In particular, a value  $T_c=80$  K for  $\text{Ge}_{0.95}\text{Mn}_{0.05}$  was anticipated by Dietl *et al.*<sup>5</sup> Recently effective pair exchange interactions in  $\text{Ge}_{1-x}\text{Mn}_x$  have also been studied ab initio.<sup>13</sup> The authors showed that the value of  $T_c$  depended on the Mn concentration, being up to 175 K at  $x=3.5\%$ . Experimentally it has been demonstrated that in epitaxial  $\text{Ge}_{1-x}\text{Mn}_x$  films  $T_c$  increases linearly with Mn concentration from 25 K to 116 K,<sup>14</sup> whereas bulk  $\text{Ge}_{0.94}\text{Mn}_{0.06}$  single crystals have been reported to have a  $T_c$  of 285 K.<sup>15</sup> Recently it has been shown that co-doping of  $\text{Ge}_{1-x}\text{Mn}_x$  by an additional transi-

tion metal, e.g., iron or cobalt, causes a significant increase both in the magnetic moment and  $T_c$ .<sup>16,17</sup> For example, the highest Curie temperature reported for co-doped epitaxial  $\text{Ge}_{100-(x+y)}\text{Mn}_x\text{Fe}_y$  films<sup>16</sup> was  $T_c=350$  K, although the possibility of phase separation was not considered in that study. Special attention has been given to group IV semiconductors due to their compatibility with existing silicon technologies. In particular, germanium is closely lattice matched to the AlGaAs family and has a higher intrinsic hole mobility than both GaAs and Si. A group IV host may also provide the simplest system for investigation of the fundamental origin of the DMS effect.

The majority of studies on DMS have focused on bulk and thin film materials, whereas the integration of DMS materials into electronics will require the manufacture of nanoscale components. There is currently an outstanding interest in the 1D semiconductor nanostructures as building units for nanoelectronic and optoelectronic. Incorporation of magnetic semiconductor nanowires with nanodevices will be the first step towards a 3D architecture of novel spintronics micro-chips.<sup>18</sup> Furthermore, nanowires provide an excellent opportunity to study the role of dimensionality and size on the magnetic properties of DMS.

Here we report the fabrication and structural and magnetic investigation of  $\text{Ge}_{1-x}\text{Mn}_x$  ( $x=1\% - 5\%$ ) nanowires with mean diameters of 35 and 60 nm. We show that the nanowires are ferromagnetic at room temperature. The dependencies of the magnetic properties of the nanowires on their diameter and Mn concentration are investigated.

### II. SAMPLE PREPARATION AND CHARACTERIZATION

Surface doped  $\text{Ge}_{1-x}\text{Mn}_x$  nanowires were synthesized within anodized aluminium oxide (AAO) templates using supercritical fluid (SCF) technique. Nanowires were fabricated through the degradation of diphenylgermane and dimanganese decacarbonyl in supercritical  $\text{CO}_2$  at 500 °C. To get a 5% Mn doped sample, 0.03 g of dimanganese decacarbonyl was premixed with 0.412 ml of diphenylgermane. The pro-

portion of dimanganese decacarbonyl was proportionately reduced to decrease the Mn content in other samples. AAO membranes with pore openings of 35 and 60 nm were used in this work. The length of the nanowires,  $L=60\ \mu\text{m}$ , is determined by the thickness of the membrane. Structural and chemical characterization of the prepared nanowires was carried out using transmission electron microscope (TEM), x-ray diffraction (XRD), x-ray photoelectron spectroscopy (XPS), extended x-ray absorption fine edge structure (EXAFS), and x-ray absorption near edge structure (XANES) techniques. The concentration of manganese within the nanowires was determined by x-ray fluorescence (XRF). The details of the preparation and characterization procedure are published elsewhere.<sup>19</sup> Magnetization measurements were performed using a commercial SQUID magnetometer (MPMS XL, Quantum Design) at temperatures between 1.8 and 370 K and in fields up to 10 kOe. A magnetic field was applied along the nanowire long axis, i.e., perpendicular to the sample surface. Correction for a diamagnetic contribution from the AAO membrane was done on all of the data. Additionally magnetic properties of a reference sample containing undoped Ge nanowires were checked. All magnetization measurements data for  $\text{Ge}_{1-x}\text{Mn}_x$  nanowires were corrected for this contribution as well.

Figure 1(a) demonstrates a high-resolution TEM image of an individual  $\text{Ge}_{0.97}\text{Mn}_{0.03}$  nanowire liberated from the membrane. The image reveals polycrystalline germanium grains with the Ge (111) lattice plane,  $d=3.3\ \text{\AA}$ . Figure 1(b) shows the powder x-ray diffraction patterns obtained from highly crystalline  $\text{Ge}_{0.97}\text{Mn}_{0.03}$  nanowires with diameter of 60 nm. The diffraction peaks observed correspond to the (111), (220), (311), (400), and (331) planes for a cubic germanium lattice. No peaks associated with the formation of metallic secondary-phase GeMn alloys were detected. Structural data show the increased Mn concentration at the nanowire-AAO membrane interface,<sup>19</sup> which was observed in the whole concentration range of manganese doping,  $x=1\% - 5\%$ . Thus, the nanowire core is Mn depleted, whereas the vicinity of the interface is rich on the magnetic impurity. Although it was not possible to determine the precise distribution of manganese atoms through the nanowire structure, EXAFS and XANES results demonstrate that Mn atoms in all of the samples investigated were surrounded by oxygen and germanium atoms rather than other neighboring Mn atoms.<sup>19</sup> The data, therefore, suggest that within an uncertainty of the used experimental techniques individual Mn atoms are well separated from each other even at the nanowire-AAO interface, where their concentration reaches its maximum. The EXAFS data also confirm the absence of magnetic alloys such as  $\text{Ge}_3\text{Mn}_5$ ,  $\text{Ge}_5\text{Mn}_3$ , and  $\text{Ge}_8\text{Mn}_{11}$ . However, the analysis of the elemental TEM mapping data suggests a small segregation of Mn at  $x=5\%$ . The effect is small and beyond the resolution limits of other structural techniques. Closer examination of  $\text{Ge}_{1-x}\text{Mn}_x$  nanowires by a bulk sensitive technique (XANES) (Ref. 19) demonstrated a mean oxidation state of  $2.70\pm 0.05$  for Mn. At the same time a surface sensitive technique (XPS) did not show any presence of  $\text{Mn}^{+2}$  state. Thus, we imply that on the nanowire surface Mn is in the +3 state, while  $\text{Mn}^{+2}$  could be present in some amount in the nanowire core.

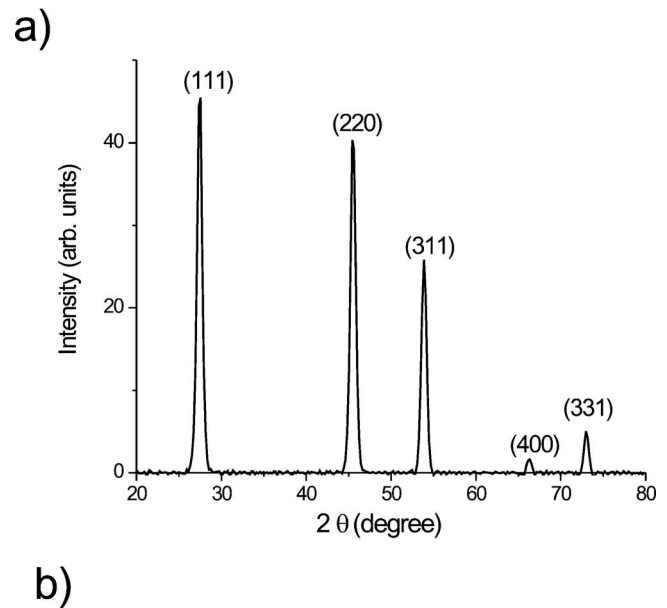
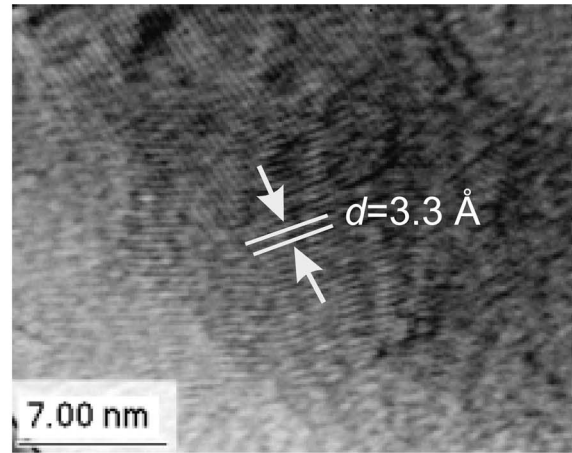


FIG. 1. (a) High-resolution TEM image of an internal region of the individual  $\text{Ge}_{0.97}\text{Mn}_{0.03}$  nanowire liberated from the AAO membrane and showing the Ge (111) lattice plane,  $d=3.3\ \text{\AA}$ . (b) XRD pattern from  $\text{Ge}_{0.97}\text{Mn}_{0.03}$  nanowires within AAO. The (111), (220), (311), (400), and (331) reflections of the cubic Ge lattice are clearly observed.

### III. MAGNETIC PROPERTIES

The effect of the dopant concentration ( $x=1\% - 5\%$ ) on the room-temperature ferromagnetism of the  $\text{Ge}_{1-x}\text{Mn}_x$  nanowires with the diameter of 35 nm is demonstrated in Fig. 2. Well-pronounced room temperature ferromagnetic properties, i.e., strongly nonlinear  $M(H)$  curves with a low field saturation and hysteresis as well as a nonzero remanence magnetization and coercivity, were observed in nanowires of this diameter at concentrations  $x\geq 1.5\%$  [Figs. 2(a)–2(c)]. The general tendency is that  $M(H)$  curves become wider and steeper as temperature decreases. The magnetization saturation is  $M_s=10-14\ \text{emu cm}^{-3}$  at  $x=1.5\%$  and  $3\%$  [Figs. 2(a) and 2(b)] and increases significantly, up to  $M_s=50.2\ \text{emu cm}^{-3}$ , at  $x=5\%$  [Fig. 2(c)]. The smallest difference in the shape and saturation value of the room- and low-

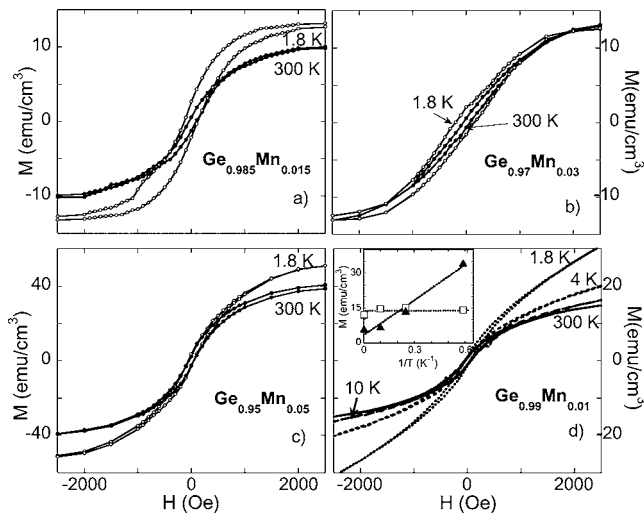


FIG. 2. Hysteresis curves for  $\text{Ge}_{1-x}\text{Mn}_x$  nanowires with the diameter of 35 nm and various concentrations of Mn ( $x=1-5\%$ ) as indicated in the figure. The inset demonstrates the temperature dependencies of para- (triangles) and ferromagnetic (squares) components of magnetization for the  $\text{Ge}_{0.99}\text{Mn}_{0.01}$  nanowire sample.

temperature curves for the nanowires with  $x=3\%$  indicates the highest  $T_c$  for this sample. The nanowires with the lowest Mn concentration ( $x=1\%$ ) demonstrate a coexistence of ferro- and paramagnetic phases, as it is illustrated in Fig. 2(d). To separate these contributions, the high-field paramagnetic input was subtracted from the original data set, and hysteresis loops with saturation ( $M_s=14 \text{ emu cm}^{-3}$ ) in low fields (not shown), typical of a ferromagnetic material, were revealed. The measured saturation field,  $H_s$ , weakly depends on temperature, being  $H_s=3 \text{ kOe}$  at 300 K and  $H_s=5 \text{ kOe}$  at  $T=10 \text{ K}$ . The inset in Fig. 2(d) illustrates the temperature dependencies of the magnetic moments of the both phases. The plot clearly demonstrates that, while the ferromagnetic component is nearly temperature independent in the investigated temperature range, the paramagnetic response is inversely proportional to the temperature, in agreement with the Curie-Weiss law for paramagnetic materials.

The concentration dependence of the coercive field is shown in Fig. 3(a), revealing a maximum at  $x=3\%$ . It is especially evident for low-temperature data, where the corresponding values of  $H_c$  increased about three times as compared with room-temperature results. The same data were plotted in Fig. 3(b) in  $H_c$  vs.  $1/T$  coordinates. The figure demonstrates that  $H_c$  increases linearly with  $1/T$  for  $x=1.5\%$  and  $3\%$  and temperature insensitive for  $x=1\%$  and  $5\%$ . Thus, the results obtained on 35 nm diameter nanowires and summarized in Figs. 2 and 3 clearly demonstrate a room-temperature ferromagnetic order of the studied nanowires, with magnetic properties being more pronounced at intermediate Mn concentrations. Unfortunately, it was not possible to study the nanowires at temperatures significantly exceeding the room temperature, therefore the exact value of  $T_c$  was not determined.

In order to prove that the magnetic properties of  $\text{Ge}_{1-x}\text{Mn}_x$  nanowires are related to Mn doping, the reference sample containing undoped Ge nanowires was prepared us-

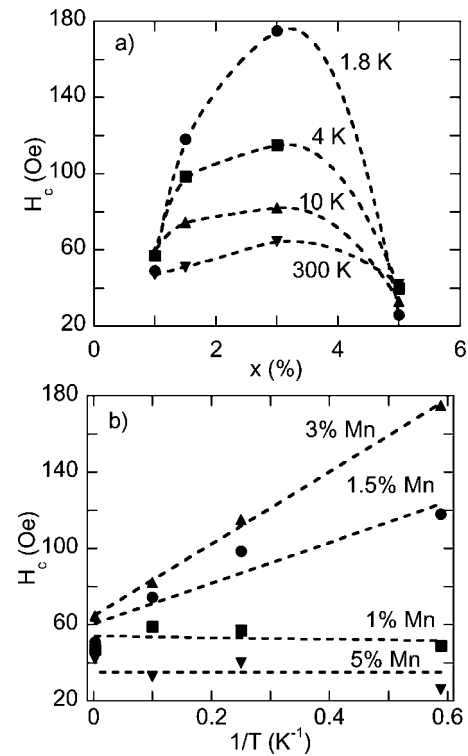


FIG. 3. Concentration (a) and temperature (b) dependencies of coercive field for arrays of 35 nm thick  $\text{Ge}_{1-x}\text{Mn}_x$  nanowires.

ing the technique described above. The reference sample showed a clear diamagnetic behavior with a negative  $M(H)$  slope even in low fields and absence of hysteresis. The magnetic moment was nearly temperature independent with a slight increase of the magnetization ( $<5\%$ ) at low temperatures, which corresponds to a presence of a small amount of uncontrolled foreign paramagnetic impurities in the AAO membrane. This fact together with convincing structural results proves that the observed soft ferromagnetism originates from Mn ions diluted in the Ge matrix, i.e.,  $\text{Ge}_{1-x}\text{Mn}_x$  nanowires exhibit a DMS type of ferromagnetic ordering.

The small nanowire diameter may cause substantial interface strain which leads to a distortion of the crystal lattice especially on the border with AAO. Such strain will unavoidably produce an increase of interfacial magnetic anisotropy which masks the magnetic properties of the system. In order to investigate qualitatively the effect of the strain,  $\text{Ge}_{1-x}\text{Mn}_x$  nanowires with a larger diameter,  $d=60 \text{ nm}$ , having a lower surface-volume ratio were studied. Magnetization as a function of magnetic field was measured in the temperature range,  $T=1.8-300 \text{ K}$ . Figure 4 shows  $M(H)$  curves for  $\text{Ge}_{0.99}\text{Mn}_{0.01}$  nanowires, i.e., the sample with the lowest Mn concentration. The curves are typical for a ferromagnetically ordered medium, i.e., saturates at  $H_s=2-7 \text{ kOe}$ , and have a rectangular shape and large coercive field,  $H_c \approx 600 \text{ Oe}$ , even at room temperature. The saturation magnetization decreases with increasing temperature and reaches only about 70% of its initial value at room temperature, while the overall type of the hysteresis curve still remains ferromagnetic. The shape of the  $M$  vs.  $H$  curves is about the same in the temperature range  $T=4-300 \text{ K}$ , whereas it is less steep in the low and

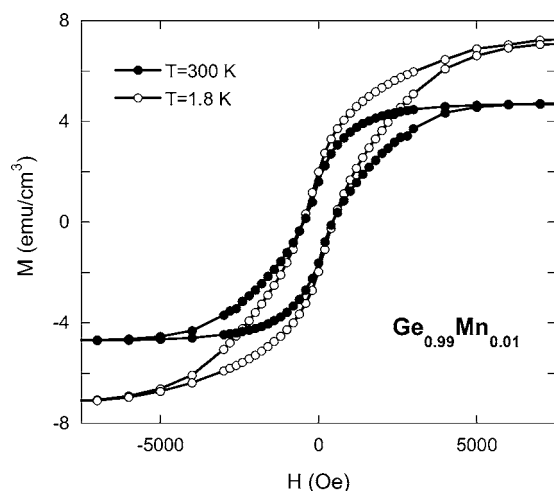


FIG. 4. Hysteresis curves for  $\text{Ge}_{0.99}\text{Mn}_{0.01}$  nanowires with the diameter of 60 nm.

intermediate fields  $0 < |H| < 4$  kOe, at  $T=1.8$  K. Thus, reducing of the interface related strain allows us to readily observe room-temperature ferromagnetism even at the lowest concentration of Mn.

#### IV. DISCUSSION

The SCF inclusion-phase technique is a relatively new method for synthesizing semiconductor nanowires. Typically such methods as chemical vapor deposition, sol-gel chemistry, and hydrothermal synthesis are commonly used. The advantages associated with the SCF technique for materials synthesis<sup>19–21</sup> allow the fabrication of  $\text{Ge}_{1-x}\text{Mn}_x$  nanowire arrays with unique magnetic properties. In particular, a Curie temperature above room temperature was observed in this study even at the lowest Mn concentration used,  $x=1\%$ . For comparison, in a thin film  $\text{Ge}_{1-x}\text{Mn}_x$  sample with a similar Mn concentration a  $T_c$  as low as 35 K was reported.<sup>14</sup>

It should be noted, that, despite relatively high growth temperatures,  $T=500$  °C, used in this work, the SCF fabrication method allows the preparation of DMS materials, which are free from undesirable phase separation and Mn clustering effects. Although formation of secondary phases is commonly observed in  $\text{Ge}_{1-x}\text{Mn}_x$  films deposited by MBE even at significantly lower temperatures, the thorough structural analysis of our samples did not reveal the presence of any GeMn alloys. A small segregation of Mn ions was shown to start at  $x=5\%$  only by means of a TEM technique, whereas all integral methods have been insensitive to this effect. In general, the small nanowire diameters within our samples should considerably reduce the probability of clustering. A similar result can be achieved in MBE-grown samples by reducing the film thickness.<sup>22</sup> Therefore, the ferromagnetism of  $\text{Ge}_{1-x}\text{Mn}_x$  nanowires investigated here cannot be explained by the formation of ferromagnetic clusters.

In all previous studies of the  $\text{Ge}_{1-x}\text{Mn}_x$  system, see e.g., Ref. 14, Mn in the Ge matrix was commonly observed in +2 state. Although a spin  $S=5/2$ ,  $L=0$ , and a magnetic moment of  $5 \mu_B$  are expectable for a  $\text{Mn}^{+2}$  ion in the substitutional

site in a Ge lattice, the electronic structure calculations<sup>14</sup> showed the strong hybridization between  $d$  states of Mn and  $p$  states of Ge which causes the reduced value of the magnetic moment of about  $3 \mu_B$  per Mn atom. It should be noted that in the present study the majority of manganese atoms are in the ionized  $\text{Mn}^{+3}$  state which is characterized by lower spin,  $S=2$ , and reduced magnetic moment ( $4 \mu_B$  per atom) compared with the  $\text{Mn}^{+2}$  state. Although the loss of a  $d$  electron in this case should give rise to an orbital momentum, detailed calculations of the  $\text{Mn}^{+3}$  electronic structure in the Ge host are required in order to determine the total momentum of Mn ions. In the concentration range  $1\% \leq x \leq 3\%$  the maximum measured saturation moment per Mn atom is about  $1.8 \mu_B$  at  $T=1.8$  K. As temperature increases, the magnetic moment per Mn atom drops to  $\approx 1.0 \mu_B$  at  $T=300$  K. The result is in good agreement with previous studies on  $\text{Ge}_{1-x}\text{Mn}_x$  (Ref. 14) and GaMnAs (Ref. 23) thin film samples. The observed low value of the magnetic moment might be explained by a generally reduced moment of  $\text{Mn}^{+3}$  ions as well as some amount of Mn ions being in a magnetically inactive state. Although EXAFS and XANES studies did not show manganese atoms in the next-neighbor positions, the formation of antiferromagnetically coupled nearest-neighbor dimers cannot be entirely excluded within an uncertainty of the experimental technique. In such configuration magnetic moments of individual ions are mutually compensated and the dimer is magnetically neutral. Thus, in this situation both Mn ions will appear magnetically inactive within the used integral experimental technique. It should be noted that a significant change in the hybridization level between  $d$  orbitals of Mn and  $p$  orbitals of the Ge host might be typical for the ionized  $\text{Mn}^{+3}$  state. In particular, weaker hybridization will lead to a weaker coupling between Mn ions and holes which makes carriers less localized and favors longer-range interactions. Overall, it may cause a room-temperature ferromagnetism observed in  $\text{Ge}_{1-x}\text{Mn}_x$  nanowires. However, detailed calculations of the electronic states in the  $\text{Ge}_{1-x}\text{Mn}_x$  system are required. A significant increase of magnetization (up to  $50 \text{ emu cm}^{-3}$  at  $T=1.8$  K) observed in  $\text{Ge}_{0.95}\text{Mn}_{0.05}$  nanowires [Fig. 2(c)] is related to the beginning of a segregation process at the high dopant concentrations.

The main question arising from our experimental data is what makes the Curie temperature in  $\text{Ge}_{1-x}\text{Mn}_x$  nanowires so high with respect to that of the bulk materials and films. Several theoretical models have been used earlier to explain a concentration dependence of the  $T_c$ . In particular, models based both on exchange interaction between carriers and localized spins<sup>5</sup> and using ab initio calculations<sup>13</sup> predicted a  $T_c$  much lower than we observe experimentally in  $\text{Ge}_{1-x}\text{Mn}_x$  nanowires. However, Park *et al.*<sup>14</sup> used a combination of electronic structure calculations based on a density-functional theory and a percolation approach to get a  $T_c = 300$  K for  $x=2\%$ . Although using this model the authors of Ref. 14 were not able to explain their own experimental results, it is the only approach which indicates a possibility of room-temperature ferromagnetism in group IV semiconductors.

As  $\text{Ge}_{1-x}\text{Mn}_x$  is a  $p$ -type semiconductor, the hole concentration plays an essential role in the mediation of ferromag-

netic ordering between localized spins of Mn atoms. Recent works on  $p$ -type semiconductors showed that  $T_c$  could be increased up and beyond room temperature if the carrier concentration is significantly raised. In particular, it was demonstrated that co-doping of GaAs:Mn by carbon leads to enhanced magnetic properties of the material, e.g., nonzero remanent magnetization was observed up to 280 K.<sup>24</sup> Carbon was shown to occupy the arsenic site and act as a shallow acceptor. Therefore, the total carrier concentration was considerably increased. Theoretically it was also predicted that it may be possible to control the magnetization and carrier density independently, by doping with Mn to supply the local magnetic moment and doping with nonmagnetic impurity to control the carrier density.<sup>25</sup> In the present work ferromagnetic ordering was observed for all samples [with an exception of the case shown in Fig. 2(d)] at room temperature. As carbon-contained precursors (diphenylgermane and dimanganese decacarbonyl) were used during the nanowire fabrication, the possibility of carbon penetration into the nanowire and especially its presence on the interface is relatively high. In the result, a hole-enriched  $\text{Ge}_{1-x}\text{Mn}_x$  could demonstrate enhanced magnetic properties due to a co-doping effect in agreement with the references above. Assuming the presence of co-dopant, the existence of single-phase ferromagnetic ordering at the lowest Mn concentration (see Fig. 4) can also be attributed to a relatively high carrier density which only partly originates from Mn doping. However, it is usually difficult to trace a small amount of carbon by standard structural techniques. Alternative approaches, e.g., measurements of carrier concentration and mobility, should be envisaged. In particular, technologically challenging Hall effect measurements on an individual nanowire would be of great interest.

As the presence of oxygen in  $\text{Ge}_{1-x}\text{Mn}_x$  nanowires was proved experimentally,<sup>19</sup> its influence on the magnetic properties cannot be excluded. For example, it was shown that in wideband GaN:Mn semiconductors addition of oxygen (8 at. %) leads to a significant enhancement of the magnetic moment.<sup>4</sup> Electronic structure calculations<sup>26</sup> have also demonstrated the significant enhancement of ferromagnetism in GaMnN with oxygen co-doping, which may as well increase  $T_c$ .

The above reasoning by analogy only suggests a possible mechanism for the high  $T_c$  in the  $\text{Ge}_{1-x}\text{Mn}_x$  system. Band structure calculations of nonmagnetic impurities, such as carbon and oxygen, in Ge should be performed taking into account the restricted dimensionality of the system. These calculations are supposed to clarify the position of co-dopant levels in the Ge host and their influence on Mn ions. Further experiments on samples with well-controlled concentration of co-dopants are also necessary to test the validity of the model and optimize the nanowire properties.

In strongly confined  $\text{Ge}_{1-x}\text{Mn}_x$  nanowires the surface-volume ratio of atoms is significantly increased compare with thin films and bulk samples. This ratio is even higher for the dopant atoms, as an enhanced Mn concentration in the nanowire shell was observed. As the host lattice is distorted in the vicinity of the membrane, the symmetry of the Mn atom environment at the interface does not correspond to that in the inner part of the nanowire. A modified crystalline

field may cause broadening of manganese wave functions and correspondingly stronger exchange in the vicinity of the interface. Thus, the AAO-nanowire interface should notably influence the electronic and magnetic properties of Mn at the nanowire shell and may lead to the high value of the Curie temperature.

Concentration dependence study reveals that the ferromagnetic behavior is most pronounced for samples with intermediate Mn concentration,  $x=1.5\%$  and  $3\%$  (Figs. 2 and 3). This is consistent with results of others, see, e.g., Ref. 14, where, despite an overall rather low Curie temperature, the maximum of  $T_c$  was reached at  $x=3.5\%$ . At the same time, D'Orazio *et al.*<sup>22</sup> demonstrated recently very similar concentration dependence with a maximum of magnetic performance at the intermediate concentration range followed by a total collapse of ferromagnetism at  $x=5.5\%$ . Our results are also consistent with earlier studies,<sup>13,14</sup> where reduction of the pair exchange interaction with increasing concentrations of the Mn atoms was observed. In the case of nanowires of small diameter and low Mn concentration [Fig. 2(d)] ferromagnetic ordering is less likely in the nanowire core as Mn ions are spaced further apart there. Thus, the central part of the nanowire is assumed to be paramagnetic due to localized magnetic ions, whereas a ferromagnetic ordering takes place in the narrow region at the border with the AAO membrane. While in the nanowire core Mn ions are likely to occupy a substitutional position, the energy of formation of both substitutional and interstitial defects is the same on the Ge interface.<sup>27</sup> In this case, the initially low concentration of carriers could be further decreased by Mn interstitial defects. Such defects act as donors, compensating a fraction of the free holes. As the concentration of Mn and carriers increases, it becomes sufficient to overcome the reducing influence of interfacial defects. Then the ferromagnetic behavior can be readily observed, though the influence of the strain is reflected in the nonsquare shape of the hysteresis [Figs. 2(a)–2(c)].

Generally the decrease of the Curie temperature with increasing mean concentration of dopants in thin films and bulk samples is believed to be connected with either the hole compensation effect or the clustering of dopants. As it is discussed above the clustering process is suppressed in the case of the nanowires due to their smaller dimensionality with respect to thin films, although a nonhomogeneous distribution of Mn ions should also be taken into account. Thus, the observed high  $T_c$  allows us to suggest suppression of both mentioned effects in the nanowire geometry.

## V. SUMMARY

We have demonstrated room-temperature ferromagnetism in the arrays of  $\text{Ge}_{1-x}\text{Mn}_x$  nanowires. Aligned crystalline  $\text{Ge}_{1-x}\text{Mn}_x$  ( $x=1\%–5\%$ ) nanowires with the smallest diameter of 35 nm were fabricated in the porous of AAO membrane. It was shown that the ferromagnetic characteristics reach their maximum at intermediate Mn concentrations followed by a qualitative change of the magnetic properties at  $x=5\%$ . The decrease of the nanowire diameter leads to the appearance of an interfacial strain which masks the ferro-

magnetic behavior. The nature of room temperature ferromagnetic behavior in the nanowires is not clearly understood, though the existence of metallic ferromagnetic GeMn alloys can be excluded. The confinement effect plays a substantial role in the system, as an oxygen-rich AAO-nanowire boundary may significantly influence the electron wave functions and the strength of the exchange interaction in the vicinity of the interface. Another possible source of room-temperature ferromagnetism is carbon co-doping of the Ge:Mn system, which may lead to a significant increase of the carrier density. Additional experiments, in particular on determination of carriers sign, density and mobility, as well as electronic structure calculations are required in order to understand the mechanism of the ferromagnetic exchange in the system.

The observation of ferromagnetic properties in Mn-doped Ge nanowires at 300 K as well as compatibility of germanium and silicon allow straightforward integration of Ge<sub>1-x</sub>Mn<sub>x</sub> nanowires into mainstream electronics and open the way for room-temperature spintronic devices.

#### ACKNOWLEDGMENTS

The authors acknowledge financial support from the QMP04.3.4 of NMS Quantum Metrology Program and the Higher Education Authority (HEA) in Ireland. We are very grateful to O. Mryasov for a fruitful discussion on the electronic structure of DMS materials and P. Josephs-Franks and J.T. Janssen for their helpful scientific comments.

---

\*Electronic address: olga.kazakova@npl.co.uk

- <sup>1</sup>G. Schmidt, *J. Phys. D* **38**, R107 (2005).
- <sup>2</sup>H. Ohno, H. Munekata, T. Penney, S. von Molnar, and L. L. Chang, *Phys. Rev. Lett.* **68**, 2664 (1992).
- <sup>3</sup>A. H. Macdonald, P. Schiffer, and N. Samarth, *Nat. Mater.* **4**, 195 (2005).
- <sup>4</sup>S. J. Pearton, C. R. Abernathy, G. T. Thaler, R. Frazier, F. Ren, A. F. Hebard, Y. D. Park, D. P. Norton, W. Tang, M. Stavola, J. M. Zavada, and R. G. Wilson, *Physica B* **340-342**, 39 (2003).
- <sup>5</sup>T. Dietl, H. Ohno, F. Matsukura, J. Cibert, and D. Ferrand, *Science* **287**, 1019 (2000).
- <sup>6</sup>M. L. Reed, N. A. El-Masry, H. H. Stadelmaier, M. K. Ritums, M. J. Reed, C. A. Parker, J. C. Roberts, and S. M. Bedair, *Appl. Phys. Lett.* **79**, 3473 (2001).
- <sup>7</sup>G. T. Thaler, M. E. Overberg, B. Gila, R. Frazier, C. R. Abernathy, S. J. Pearton, J. S. Lee, S. Y. Lee, Y. D. Park, Z. G. Khim, J. Kim, and F. Ren, *Appl. Phys. Lett.* **80**, 3964 (2002).
- <sup>8</sup>S. Dhar, O. Brandt, A. Trampert, L. Daweritz, K. J. Friedland, K. H. Ploog, J. Keller, B. Beschoten, and G. Guntherodt, *Appl. Phys. Lett.* **82**, 2077 (2003).
- <sup>9</sup>A. F. Hebard, R. P. Rairigh, J. G. Kelly, S. J. Pearton, C. R. Abernathy, S. N. G. Chu, and R. G. Wilson, *J. Phys. D* **37**, 511 (2004).
- <sup>10</sup>S. J. Pearton, C. R. Abernathy, G. T. Thaler, R. M. Frazier, D. P. Norton, F. Ren, Y. D. Park, J. M. Zavada, I. A. Buyanova, W. M. Chen, and A. F. Hebard, *J. Phys.: Condens. Matter* **16**, R209 (2004).
- <sup>11</sup>F. L. Deepak, P. V. Vanitha, A. Govindaraj, and C. N. R. Rao, *Chem. Phys. Lett.* **374**, 314 (2003).
- <sup>12</sup>D. S. Han, J. Park, K. W. Rhie, S. Kim, and J. Chang, *Appl. Phys. Lett.* **86**, 032506 (2005).
- <sup>13</sup>J. Kudrnovsky, I. Turek, V. Drchal, F. Maca, P. Weinberger, and P. Bruno, *Phys. Rev. B* **69**, 115208 (2004).
- <sup>14</sup>Y. D. Park, A. T. Hanbicki, S. C. Erwin, C. S. Hellberg, J. M. Sullivan, J. E. Mattson, T. F. Ambrose, A. Wilson, G. Spanos, and B. T. Jonker, *Science* **295**, 651 (2002).
- <sup>15</sup>S. Cho, S. Choi, S. C. Hong, Y. Kim, J. B. Ketterson, B. J. Kim, Y. C. Kim, and J. H. Jung, *Phys. Rev. B* **66**, 033303 (2002).
- <sup>16</sup>H. Braak, R. R. Gareev, D. E. Bürgler, R. Schreiber, P. Grünberg, and C. M. Schneider, *J. Magn. Magn. Mater.* **286**, 46 (2005).
- <sup>17</sup>F. Tsui, L. He, L. Ma, A. Tkachuk, Y. S. Chu, K. Nakajima, and T. Chikyow, *Phys. Rev. Lett.* **91**, 177203 (2003).
- <sup>18</sup>Y. Wu, J. Xiang, C. Yang, W. Lu, and C. M. Lieber, *Nature (London)* **430**, 61 (2004).
- <sup>19</sup>J. S. Kulkarni, O. Kazakova, D. Erts, M. Morris, M. T. Shaw, and J. D. Holmes, *Chem. Mater.* **17**, 3615 (2005).
- <sup>20</sup>J. D. Holmes, D. M. Lyons, and K. J. Ziegler, *Chem.-Eur. J.* **9**, 2144 (2003).
- <sup>21</sup>K. J. Ziegler, B. Polyakov, J. S. Kulkarni, T. A. Crowley, K. M. Ryan, M. A. Morris, D. Erts, and J. D. Holmes, *J. Mater. Chem.* **14**, 585 (2004).
- <sup>22</sup>F. D'Orazio, F. Lucari, N. Pinto, L. Morresi, and R. Murri, *J. Magn. Magn. Mater.* **272-276**, 2006 (2004).
- <sup>23</sup>H. Ohldag, V. Solinus, F. U. Hillebrecht, J. B. Goedkoop, M. Finazzi, F. Matsukura, and H. Ohno, *Appl. Phys. Lett.* **76**, 2928 (2000).
- <sup>24</sup>Y. D. Park, J. D. Lim, K. S. Suh, S. B. Shim, J. S. Lee, C. R. Abernathy, S. J. Pearton, Y. S. Kim, Z. G. Khim, and R. G. Wilson, *Phys. Rev. B* **68**, 085210 (2003).
- <sup>25</sup>T. Jungwirth, J. Masek, J. Sinova, and A. H. MacDonald, *Phys. Rev. B* **68**, 161202(R) (2003).
- <sup>26</sup>E. Kulatov, H. Nakayama, H. Mariette, H. Ohta, and Yu. A. Uspekii, *Phys. Rev. B* **66**, 045203 (2002).
- <sup>27</sup>X. Luo, S. B. Zhang, and S. -H. Wei, *Phys. Rev. B* **70**, 033308 (2004).